

**A total sky cloud detection method using real clear sky background**

J. Yang et al.

This discussion paper is/has been under review for the journal Atmospheric Measurement Techniques (AMT). Please refer to the corresponding final paper in AMT if available.

# A total sky cloud detection method using real clear sky background

J. Yang<sup>1,2</sup>, Q. Min<sup>2,3</sup>, W. Lu<sup>1</sup>, Y. Ma<sup>1</sup>, W. Yao<sup>1</sup>, T. Lu<sup>1</sup>, J. Du<sup>3</sup>, and G. Liu<sup>4</sup>

<sup>1</sup>State Key Laboratory of Severe Weather, Chinese Academy of Meteorological Sciences, Beijing 100081, China

<sup>2</sup>Atmospheric Sciences Research Center, State University of New York, Albany, NY 12203, USA

<sup>3</sup>School of Remote Sensing and Information Engineering, Wuhan University, Wuhan 430079, China

<sup>4</sup>Smart Grid Operation Research Center, China Electric Power Research Institute, Beijing 100192, China

Received: 6 November 2015 – Accepted: 2 December 2015 – Published: 10 December 2015

Correspondence to: Q. Min (qmin@albany.edu)

Published by Copernicus Publications on behalf of the European Geosciences Union.

Title Page

Abstract

Introduction

Conclusions

References

Tables

Figures



Back

Close

Full Screen / Esc

Printer-friendly Version

Interactive Discussion



## Abstract

The brightness distribution of sky background is usually non-uniform, which creates many problems for traditional cloud detection methods including the failure of thin cloud detection in total sky images and significantly reducing retrieval accuracy in the circum-solar and near-horizon regions. This paper describes the development of a new cloud detection algorithm, named “clear sky background differencing (CSBD)”, which is accomplished by differencing the original image and the corresponding clear sky background image using the images’ green channel. First, a library of clear sky background images with a variety of solar elevation angles needs to be developed. The image rotation and image brightness adjustment algorithms are applied to ensure the two images being differenced have the same solar position and similar brightness distribution. Sensitivity tests show, as long as the positions of the sun in the two images are the same, the cloud detection results are satisfactory. Several experimental cases show that the CSBD algorithm obtains good cloud recognition results visually, especially for thin clouds.

## 1 Introduction

Clouds are an essential part of the atmospheric energy and water cycle, and their coverage state is crucial for radiative transfer models and climate simulations. Traditional visual observations have been carried out worldwide at meteorological stations to estimate sky cloud amount for more than 100 years (Deutscher Wetterdienst, 2013). So far, human observations are still the main means to obtain surface cloud coverage in many countries. However, the subjectivity of visual observations introduces significant uncertainty into cloud coverage measurement accuracy. In the Automated Surface Observing Systems (ASOS) program, a laser ceilometer is widely used, instead of visual observations, to retrieve whole sky cloud amount based on a time series of ceilometer data. The more direct means of determining cloud cover is using a digital camera and

### A total sky cloud detection method using real clear sky background

J. Yang et al.

Title Page

Abstract

Introduction

Conclusions

References

Tables

Figures



Back

Close

Full Screen / Esc

Printer-friendly Version

Interactive Discussion













for any two different imaging times. This is a big challenge for us to establish the CSBL. If we build the CSBL included the CSB images for all times, the database will be too large and complex.

Fortunately, using the symmetry of the total sky images (Huo and Lu, 2009), we can rotate each TCI image along the center of the image and the center of the sun, where the rotation angle is equal to the solar azimuth. Figure 3a and b are two TCI images acquired on the A.M. and P.M. of 8 October 2012, respectively. Obviously, the positions of the sun in these two images are completely different, though they have the same solar elevation angles; one is on the right of the image, and the other is on the left. After image rotation, the centers of the sun in the two images (see the Fig. 3e and f) are almost completely coincident. Here, to better preserve the brightness information of the original images, the nearest-neighbor interpolation algorithm is adopted when performing image rotation. Another two TCI images (Fig. 3c and d) are captured at different dates. They also have the same solar elevation angles but different solar azimuth angles, resulting in entirely different coordinates of the sun between the two images. Figure 3g and h show the results after image rotation, in which the positions of two solar centers are exactly the same. Actually, the four TCI images (Fig. 3a–d) have equal solar elevation angles. Using the technique of image rotation, the CSB for these four times in the CSBL can be represented using any one of Fig. 3e–h.

Every day the sun rises from the east and sets in the west, and the solar azimuth angle and the solar elevation angle change constantly. For any TCI image, by rotating the image with an angle equal to the solar azimuth, the sun will always be situated at the lower half of the perpendicular bisector of the image. The distance from the center of the sun to the center of the image is determined by the solar elevation angle, so we build a database representing the real clear sky background with different solar elevation angles. The interval of the solar elevation angles in the CSBL is  $1^\circ$ . Figure 4 shows examples of the CSBL for some typical CSB images, which were captured on 11 June 2013. The CSBL is updated on every clear sky day through the year because aerosols and climate affect the brightness distribution of the clear sky. Therefore, when

## A total sky cloud detection method using real clear sky background

J. Yang et al.

Title Page

Abstract

Introduction

Conclusions

References

Tables

Figures



Back

Close

Full Screen / Esc

Printer-friendly Version

Interactive Discussion





For some thin clouds, this method can also give an accurate identification. Even some bright noises, caused by the refraction of the light, are successfully excluded from the detection result because of their constant positions and similar brightness in the Fig. 5e and f.

### 3.4 Sensitivity tests

The theoretical basis of the proposed CSBD algorithm is that two images have similar brightness distribution as long as the positions of the sun in the images are the same. So a correct CSB image is critical for the accurate cloud detection. To check the influence of the CSB images with different solar elevation angles on our algorithm, we performed some sensitivity tests. Figure 6 shows the cloud detection results for a TCI image based on different CSB images. Figure 6a is the original TCI image after rotation, which was taken on 11 October 2012, with its solar elevation angle equal to  $33^\circ$ . Figure 6b represents three different CSB images. Figure 6c is the resulting difference images, and Fig. 6d is the corresponding cloud detection results. The CSB image in the first row has the completely same solar elevation angle as Fig. 6a, while the solar elevation angle of the CSB image in the second row deviates  $2^\circ$  from the Fig. 6a, and the deviation of solar elevation angle in the last row is  $5^\circ$ . It is obvious that the cloud detection result in the first row is better than the others because the CSB image in that row has identical solar elevation angles with Fig. 6a. When there is a deviation of solar elevation angle between the two images, some cloud detection errors will appear, especially in the circumsolar region. The greater the deviation angle, the greater the cloud detection errors.

Figure 7 shows the cloud detection results for the other TCI image based on different CSB images. The design and the test are the same as in Fig. 6, but the TCI image in the Fig. 7a was acquired on 20 March 2013 and its solar elevation angle is equal to  $50^\circ$ , which is higher than in the Fig. 6a. The test results for another TCI image are given in the Fig. 8. Different from the first two tests, the TCI image in the Fig. 8a was obtained on 28 June 2013, and has a very high solar elevation angle (about  $65^\circ$ ). The conclusions

## A total sky cloud detection method using real clear sky background

J. Yang et al.

Title Page

Abstract

Introduction

Conclusions

References

Tables

Figures



Back

Close

Full Screen / Esc

Printer-friendly Version

Interactive Discussion





## 4 Results comparison

To better understand the effectiveness of the proposed CSBD method, the cloud detection results for five different TCI images, using different methods, are compared in Fig. 10. In this comparison, we selected three traditional algorithms as references, including 2-D R/B, 3-D multi-color, and 1-D GBSAT. For the 2-D R/B method, 0.6 is adopted as a single threshold. Figure 10a shows the original TCI images after rotation, Fig. 10b is the results of 2-D R/B method, Fig. 10c represents the results of 3-D multi-color method, Fig. 10d presents the results of 1-D GBSAT algorithm, and the last column of Fig. 10 is the results of CSBD algorithm. Of all these results, the white pixels represent cloud and black pixels are sky regions.

Quantitatively evaluating the precision of different cloud detection methods is considerably difficult because, if we want to carry out such an assessment, a standard cloud mask for each TCI image first needs to be available. However, such a standard mask can only be obtained by manual sketch and, as such, is heavily dependent on human objectivity. So, in this comparison, we simply evaluate the precision of different cloud detection methods by visual examination. The results of 2-D R/B method are acceptable for some thick clouds but unacceptable for the vast majority of thin clouds. When the sun is visible in the TCI images, the 2-D R/B method misclassifies most of sun pixels into cloud pixels. Of all these algorithms, the 3-D multi-color method incorrectly identified the most sky pixels as cloud pixels, especially in the circumsolar and near-horizon regions. The reason may be that some fixed multi-color criteria are not suitable for our TCI instruments and local climatic conditions. The GBSAT algorithm obtains satisfactory results, both in the circumsolar and near-horizon regions, but still fails to detect some thin clouds, as seen in the last two rows for the fourth column. The CSBD algorithm outperforms the traditional methods, especially when the sun is visible. The results of these cases also indicate the CSBD algorithm is very effective for thin clouds, for which it can obtain better results than the classical methods. The bright

### A total sky cloud detection method using real clear sky background

J. Yang et al.

Title Page

Abstract

Introduction

Conclusions

References

Tables

Figures



Back

Close

Full Screen / Esc

Printer-friendly Version

Interactive Discussion







## A total sky cloud detection method using real clear sky background

J. Yang et al.

Title Page

Abstract

Introduction

Conclusions

References

Tables

Figures



Back

Close

Full Screen / Esc

Printer-friendly Version

Interactive Discussion



- Heinle, A., Macke, A., and Srivastav, A.: Automatic cloud classification of whole sky images, *Atmos. Meas. Tech.*, 3, 557–567, doi:10.5194/amt-3-557-2010, 2010.
- Huo, J. and Lu, D.: Cloud determination of all-sky images under low visibility conditions, *J. Atmos. Ocean. Tech.*, 26, 2172–2180, 2009.
- 5 Kazantzidis, A., Tzoumanikas, P., Bais, A. F., Fotopoulos, S., and Economou, G.: Cloud detection and classification with the use of whole-sky ground-based images, *Atmos. Res.*, 113, 80–88, 2012.
- Kimmel, R.: Demosaicing: imaging reconstruction from color CCD samples, *IEEE T. Image Process.*, 8, 1221–1228, 1999.
- 10 Klebe, D. I., Blatherwick, R. D., and Morris, V. R.: Ground-based all-sky mid-infrared and visible imagery for purposes of characterizing cloud properties, *Atmos. Meas. Tech.*, 7, 637–645, doi:10.5194/amt-7-637-2014, 2014.
- Koehler, T. L., Johnson, R. W., and Shields, J. E.: Status of the Whole Sky Imager Database, in: *Proc. Cloud Impacts on DOD Operations and Systems*, Department of Defense, El Segundo, California, USA, 77–80, 1991.
- 15 Li, Q., Lu, W., and Yang, J.: A hybrid thresholding algorithm for cloud detection on ground-based color images, *J. Atmos. Ocean. Tech.*, 28, 1286–1296, 2011.
- Long, C. N.: Correcting for circumsolar and near-horizon errors in sky cover retrievals from sky images, *Open Atmos. Sci. J.*, 4, 45–52, 2010.
- 20 Long, C. N. and Deluisi, J. J.: Development of an automated hemispheric sky imager for cloud fraction retrievals, in: *Proc. 10th Symp. on Meteorological Observations and Instrumentation*, Phoenix, Arizona, USA, 11–16 January 1998, 171–174, 1998.
- Long, C. N., Sabburg, J. M., Calbo, J., and Pagès, D.: Retrieving cloud characteristics from ground-based daytime color all-sky images, *J. Atmos. Ocean. Tech.*, 23, 633–652, 2006.
- 25 Meeus, J.: *Astronomical Algorithms*, 2nd edn., Willmann-Bell Inc., Virginia, USA, 1998.
- Michalsky, J. J.: The astronomical Almanac's algorithm for approximate solar position (1950–2050), *Sol. Energy*, 40, 227–235, 1988.
- Shields, J. E., Johnson, R. W., and Koehler, T. L.: Automated whole sky imaging systems for cloud field assessment, in: *Fourth Symposium of Global Change Studies*, 17–22 January 1993, American Meteorological Society, Boston, Massachusetts, USA, 228–231, 1993.
- 30 Souza-Echer, M. P., Pereira, E. B., Bins, L. S., and Andrade, M. A. R.: A simple method for the assessment of the cloud cover state in high-latitude regions by a ground-based digital camera, *J. Atmos. Ocean. Tech.*, 23, 437–447, 2006.

## A total sky cloud detection method using real clear sky background

J. Yang et al.

Title Page

Abstract

Introduction

Conclusions

References

Tables

Figures



Back

Close

Full Screen / Esc

Printer-friendly Version

Interactive Discussion



- Spencer, J. M.: Fourier series representation of the position of the sun, *Search*, 2, p. 172, 1971.
- Sylvio, L. M. N., Wangenheim, A. V., Pereira, E. B., and Comunello, E.: The use of Euclidean geometric distance on RGB color space for the classification of sky and cloud patterns, *J. Atmos. Ocean. Tech.*, 27, 1504–1517, 2010.
- 5 Yamashita, M. and Yoshimura, M.: Ground-based cloud observation for satellite-based cloud discrimination and its validation, in: *International Archives of the Photogrammetry, Remote Sensing and Spatial Information Sciences, Volume XXXIX-B8, XXII ISPRS Congress, 25 August–1 September 2012, Melbourne, Australia*, 137–140, 2012.
- Yang, J., Lu, W., Ma, Y., and Yao, W.: An automated cirrus cloud detection method for a ground-
- 10 based cloud image, *J. Atmos. Ocean. Tech.*, 29, 527–537, 2012.
- Yang, J., Min, Q., Lu, W., Yao, W., Ma, Y., Du, J., Lu, T., and Liu, G.: An automated cloud detection method based on the green channel of total-sky visible images, *Atmos. Meas. Tech.*, 8, 4671–4679, doi:10.5194/amt-8-4671-2015, 2015.

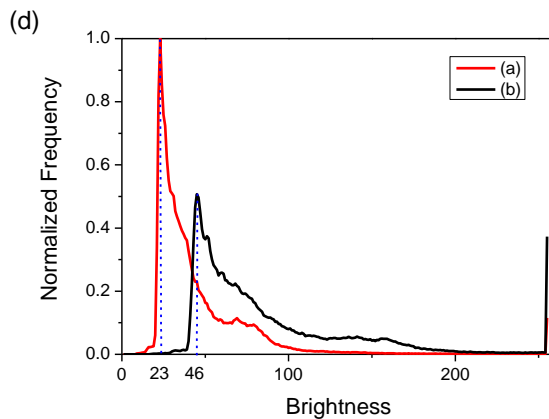
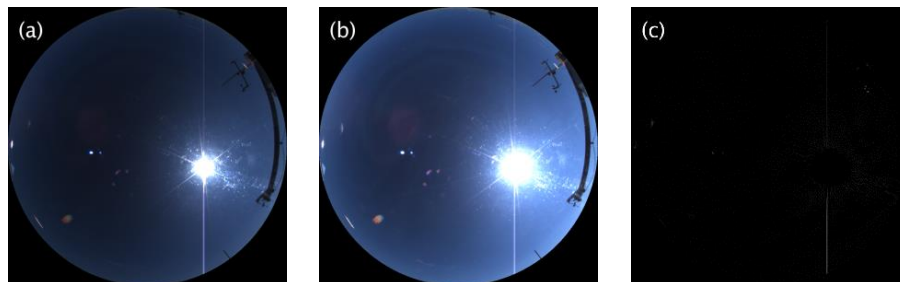


**Figure 1.** Relationships between the exposure time and the brightness value for the TCI images. **(a)** TCI image at exposure time of  $300\ \mu\text{s}$ , **(b)** TCI image with the same lighting conditions and camera parameters as in **(a)**, but with  $600\ \mu\text{s}$  exposure time, **(c)** difference of  $2\times$  **(a)** and **(b)** for the green channel, and **(d)** normalized brightness histograms distribution for the green channel of **(a)** and **(b)**.

**A total sky cloud detection method using real clear sky background**

J. Yang et al.

Title Page

Abstract

Introduction

Conclusions

References

Tables

Figures

◀

▶

◀

▶

Back

Close

Full Screen / Esc

Printer-friendly Version

Interactive Discussion



## A total sky cloud detection method using real clear sky background

J. Yang et al.

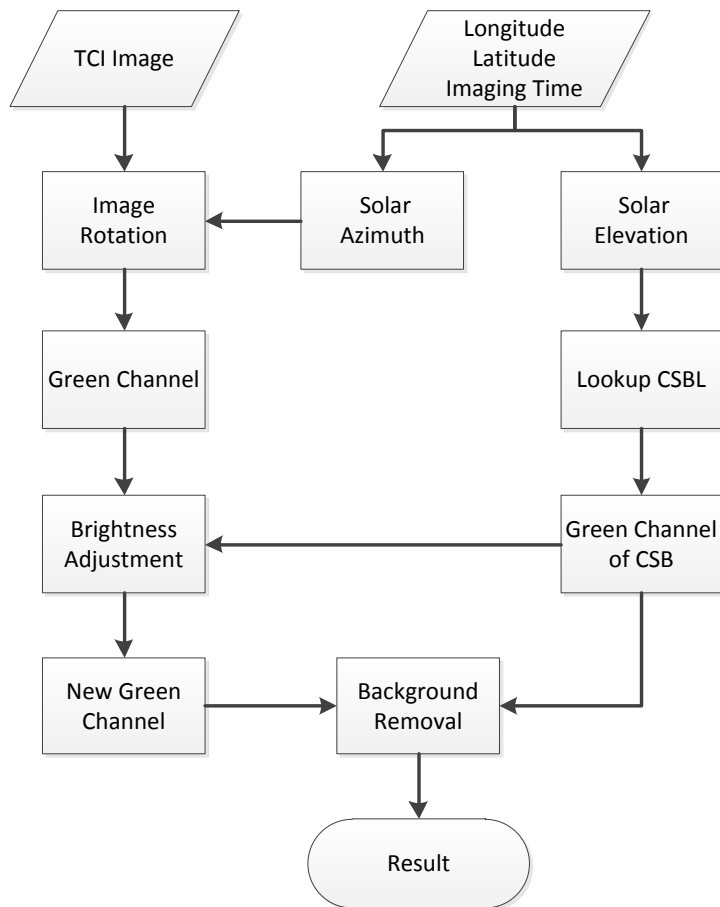


**Figure 2.** Flowchart of the proposed algorithm.

Title Page

Abstract Introduction

Conclusions References

Tables Figures

◀ ▶

◀ ▶

Back Close

Full Screen / Esc

Printer-friendly Version

Interactive Discussion



## A total sky cloud detection method using real clear sky background

J. Yang et al.

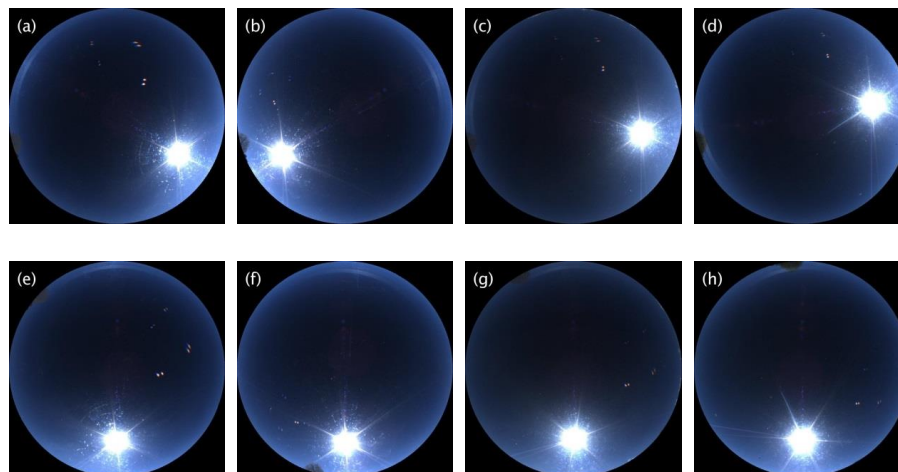


**Figure 3.** Several TCI images of different imaging times and the results after rotation. **(a)** and **(b)** are the TCI images shot on the A.M. and P.M. of 8 October 2012, respectively, **(c)** is captured on 5 April 2013, **(d)** is obtained on 11 June 2013, with **(e)** through **(h)** as the corresponding rotation images of **(a)** to **(d)**.

[Title Page](#)[Abstract](#)[Introduction](#)[Conclusions](#)[References](#)[Tables](#)[Figures](#)[◀](#)[▶](#)[◀](#)[▶](#)[Back](#)[Close](#)[Full Screen / Esc](#)[Printer-friendly Version](#)[Interactive Discussion](#)

## A total sky cloud detection method using real clear sky background

J. Yang et al.

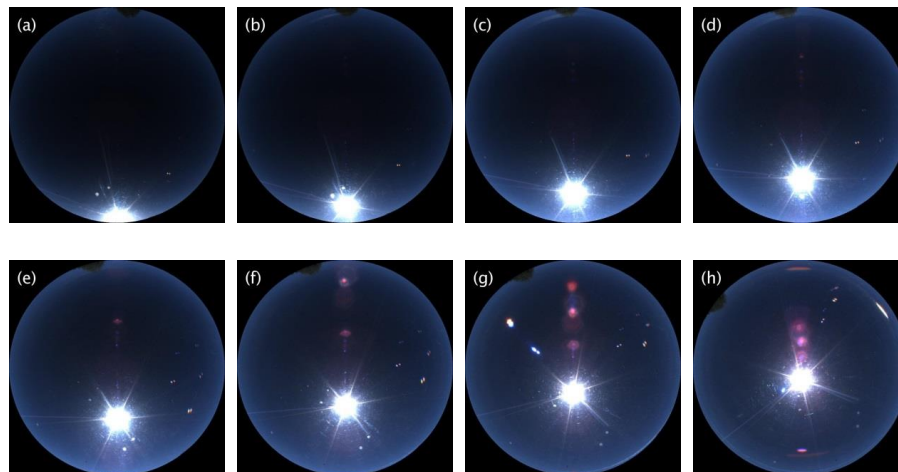


**Figure 4.** Several typical clear sky background images captured on 11 June 2013. The solar elevation angles of (a) to (h) are range from 10 to 80° at intervals of 10°.

[Title Page](#)[Abstract](#)[Introduction](#)[Conclusions](#)[References](#)[Tables](#)[Figures](#)[◀](#)[▶](#)[◀](#)[▶](#)[Back](#)[Close](#)[Full Screen / Esc](#)[Printer-friendly Version](#)[Interactive Discussion](#)

## A total sky cloud detection method using real clear sky background

J. Yang et al.

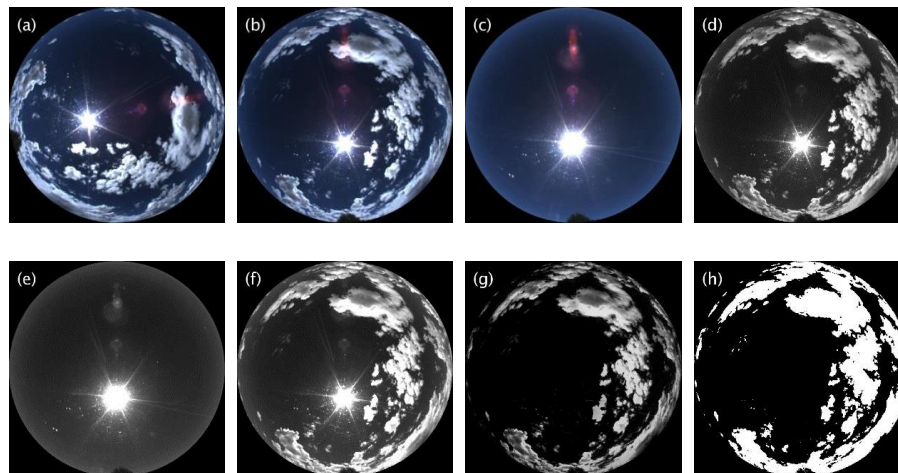


**Figure 5.** Cloud detection result based on CSB. **(a)** is the original TCI image captured on 7 June 2013, **(b)** is the image after rotation, **(c)** is the real clear background library image with the same solar elevation angle as **(b)**, **(d)** shows the green channel of **(b)**, **(e)** shows the green channel of **(c)**, **(f)** represents the new green channel of **(d)** after brightness adjustment, which has very similar brightness distribution with **(e)** especially for sky background, **(g)** is the difference of **(f)** and **(e)**, **(h)** is the ultimate cloud detection result.

Title Page

Abstract

Introduction

Conclusions

References

Tables

Figures

◀

▶

◀

▶

Back

Close

Full Screen / Esc

Printer-friendly Version

Interactive Discussion



## A total sky cloud detection method using real clear sky background

J. Yang et al.

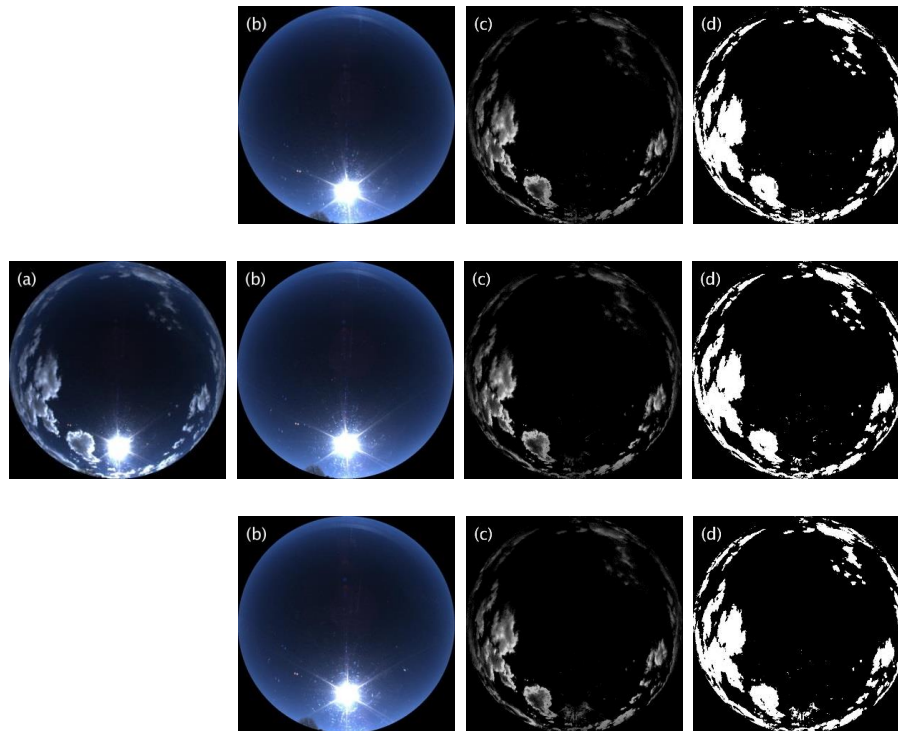


**Figure 6.** Sensitivity test for low solar elevation angle. **(a)** is the TCI image after rotation, which was captured on 11 October 2012, **(b)** is the CSB images, where the first row has the completely same solar elevation angle as **(a)**, the solar elevation angle of the second row has  $2^\circ$  deviation with **(a)**, and the solar elevation angle of the third row has  $5^\circ$  deviation with **(a)**, **(c)** is the difference images, and **(d)** is the corresponding cloud detection results.

Title Page

Abstract

Introduction

Conclusions

References

Tables

Figures

◀

▶

◀

▶

Back

Close

Full Screen / Esc

Printer-friendly Version

Interactive Discussion



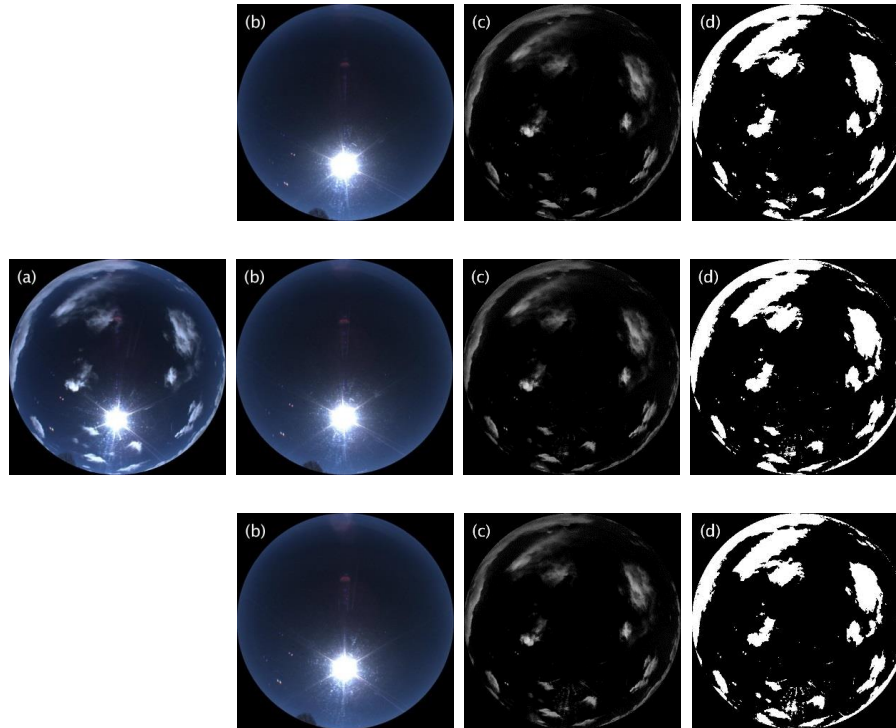


**Figure 7.** Sensitivity test as Fig. 6 but for medium solar elevation angle. **(a)** is the TCI image after rotation, which was captured on 20 March 2013, **(b)** is the CSB images, where the first row has the completely same solar elevation angle as **(a)**, the solar elevation angle of the second row has  $2^\circ$  deviation with **(a)**, and the solar elevation angle of the third row has  $5^\circ$  deviation with **(a)**, **(c)** is the difference images, and **(d)** is the corresponding cloud detection results.

**A total sky cloud detection method using real clear sky background**

J. Yang et al.

Title Page	
Abstract	Introduction
Conclusions	References
Tables	Figures
◀	▶
◀	▶
Back	Close
Full Screen / Esc	
Printer-friendly Version	
Interactive Discussion	



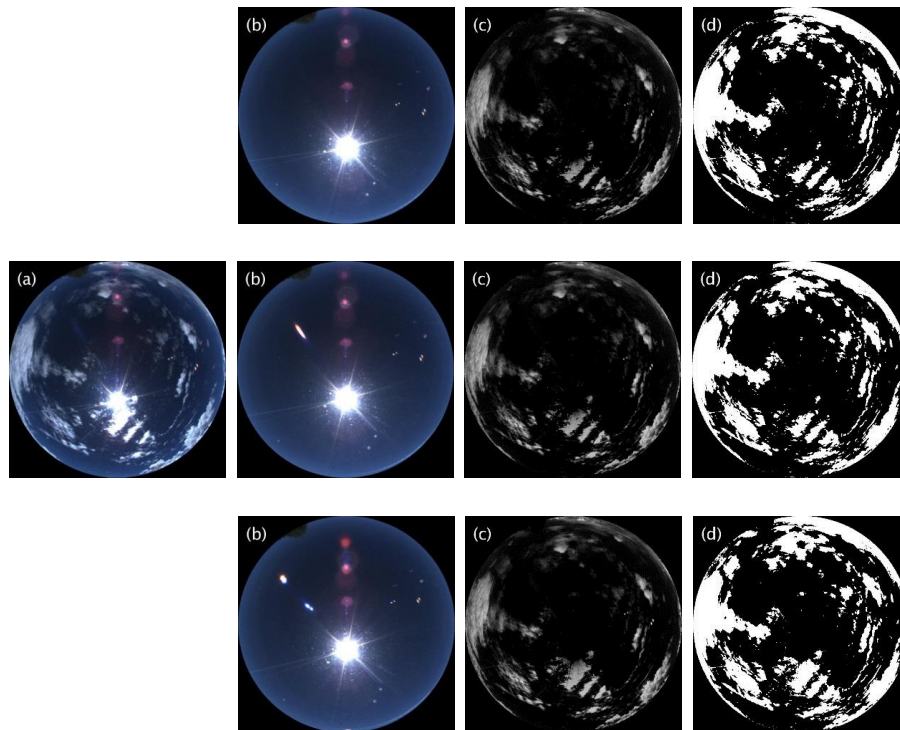


**Figure 8.** Sensitivity test as Fig. 6 but for high solar elevation angle. **(a)** is the TCI image after rotation, which was obtained on 28 June 2013, **(b)** is the CSB images, where the first row has the completely same solar elevation angle as **(a)**, the solar elevation angle of the second row has  $2^\circ$  deviation with **(a)**, and the solar elevation angle of the third row has  $5^\circ$  deviation with **(a)**, **(c)** is the difference images, and **(d)** is the corresponding cloud detection results.

## A total sky cloud detection method using real clear sky background

J. Yang et al.

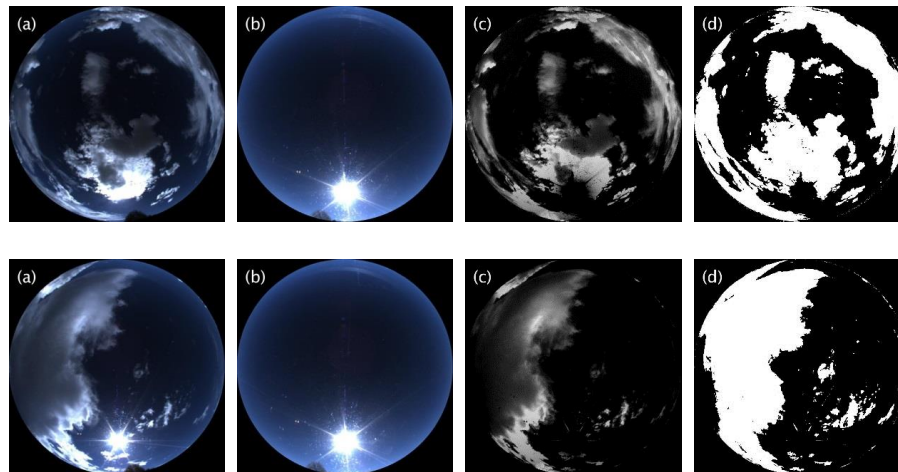


**Figure 9.** The limitations of the proposed method. **(a)** is the TCI images after rotation, **(b)** is the corresponding CSB images, **(c)** is the difference images, and **(d)** represents the final cloud detection results.

[Title Page](#)[Abstract](#)[Introduction](#)[Conclusions](#)[References](#)[Tables](#)[Figures](#)[◀](#)[▶](#)[◀](#)[▶](#)[Back](#)[Close](#)[Full Screen / Esc](#)[Printer-friendly Version](#)[Interactive Discussion](#)

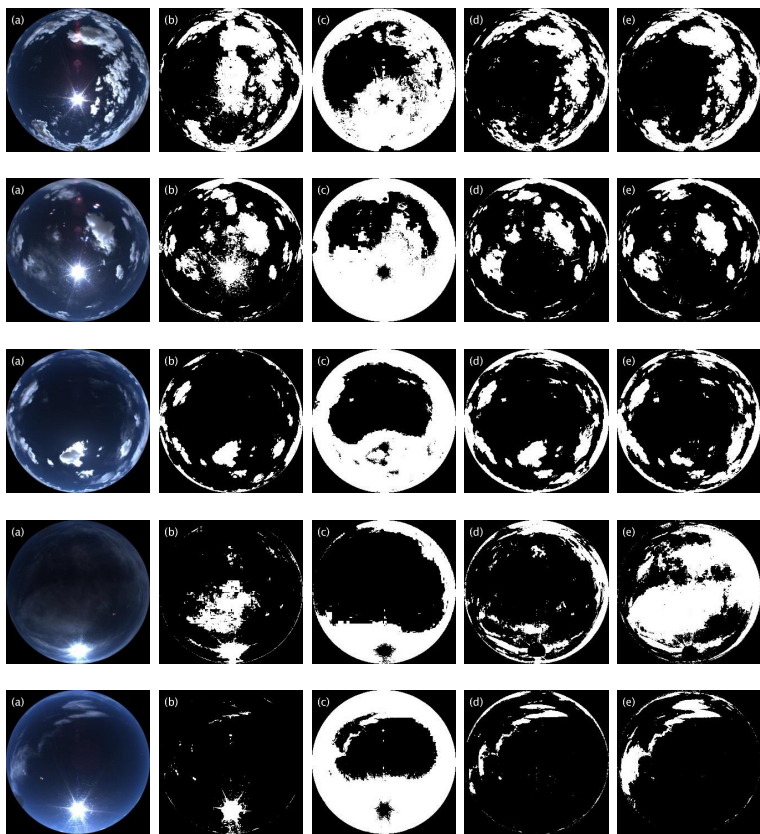


**Figure 10.** Comparison for different cloud detection methods. **(a)** is the TCI images after rotation, **(b)** represents the results of R/B, **(c)** is the results of multi-color method, **(d)** denotes the results of GBSAT, and **(e)** is the results of the proposed CSBD method.

## A total sky cloud detection method using real clear sky background

J. Yang et al.

Title Page	
Abstract	Introduction
Conclusions	References
Tables	Figures
◀	▶
◀	▶
Back	Close
Full Screen / Esc	
Printer-friendly Version	
Interactive Discussion	

